Effective sources: removing the near surface from the VSP FWI problem

Scott Keating, Matt Eaid and Kris Innanen

ABSTRACT

For land seismic surveys, the near-surface is often highly variable, resulting in a complex, substantial impact on data. This can make full-waveform inversion very difficult to apply on land seismic data sets, as accurate characterization of the near-surface can be extremely challenging. To cope with this challenge, we propose a full-waveform inversion strategy for removing the near-surface from the inversion problem in the case of vertical seismic profile data. To remove the near-surface from the inversion, we invert for both a subsurface model and a wavefield at a depth below the near-surface. In synthetic examples, we demonstrate that the inversion can accurately characterize the subsurface in this type of approach.

INTRODUCTION

Vertical seismic profiles (VSP) are a form of seismic survey design in which geophysical sensors are arrayed down a wellbore while seismic sources are deployed at the surface. This type of acquisition offers the potential for high quality seismic data to be gathered in the vicinity of a well, with many potential applications, including reservoir monitoring. The wavemodes that VSP data provides make it an interesting candidate for the use of full-waveform inversion (FWI). In surface seismic acquisition geometries, diving waves provide the key contribution to FWI through their sensitivity to the low wavenumber features of the subsurface, while reflections are typically much more difficult to use effectively (e.g. Brossier et al., 2015). In VSP surveys, the direct waves from sources to receivers provide the same type of low wavenumber coverage without the need for the very long offsets required in surface acquisition geometries.

When considering land seismic surveys, another key advantage of VSP data is the reduced impact of the near surface. Because the near surface can be highly heterogeneous and very low velocity, it can have a large impact on seismic data, and, due to its proximity to the sources, it can be very difficult to characterize. In full-waveform inversion, the driver of the inversion process is a numerical optimization procedure designed to determine the subsurface model providing synthetic data best matching the measured data. A complex near-surface can significantly complicate this effort because of the difficulties that exist in accurately characterizing it and the significant impact it has on seismic data. Because VSP surveys primarily measure raypaths with only one pass through the near-surface, they somewhat mitigate the impact of the near-surface on the measurements and inversion as compared to surface seismic surveys (which primarily measure raypaths with both a downgoing and an upgoing interaction with the near surface). This simpler interaction can also allow for different strategies for coping with the near-surface to be brought to bear.

In this report, we propose a strategy for FWI of VSP data sets where the effects of the near-surface are significant. In this approach, we eliminate the need to characterize the

near-surface by replacing each surface source used in the data acquisition with an effective source at depth. In effect, this formulation replaces the problem of characterizing a complex, heterogeneous near surface given a known source term with the problem of characterizing the wavefield produced by the interaction of the two at a chosen depth. The latter problem has the advantage of requiring an inversion for a term with a much simpler relation to the borehole measurements. In this report, we include synthetic examples demonstrating the approach. In two companion reports (Keating et al., 2021; Eaid et al., 2021a), we demonstrate that this reformulation has the potential to make the inversion problem substantially more tractable for a real VSP data set.

THEORY

A conventional FWI objective function is given by

$$\phi = \frac{1}{2}||Ru - d||_2^2 \text{ subject to } S(m)u = f., \tag{1}$$

where R is a matrix applying the receiver sampling, d are the measured data, u is a wavefield, S is a Helmholtz matrix, representing a finite-difference approximation of the frequency domain wave equation, m is a model vector, characterizing the properties of the subsurface, and f is a source term. Equation 1 describes an L_2 objective function; formulations using different objective functions will typically replace the expression for ϕ, but not the wavefield condition. In most formulations of FWI, only the subsurface model, m is treated as unknown in the inversion, but more general FWI problems, including those inverting for, for instance, the source vector, f, can be formulated (e.g. Keating and Innanen, 2020). In land FWI, there is a significant concern that the portion of m that characterizes the near-surface may be both very low velocity (necessitating a very fine finite-difference mesh and increased computational cost), and highly heterogeneous (possibly on a scale too small for our finite-difference mesh to characterize). This can result in a situation in which the near surface 1) has a very large impact on our measured data, 2) necessitates greater computational costs, and 3) typically cannot be accurately characterized in inversion. These problems are especially significant given the fact that, in most cases, a characterization of the near-surface is not, in itself, a goal of the inversion. For this reason, we suggest a reformulation of the VSP FWI problem that does not explicitly treat the specifics of near-surface seismic wave propagation.

In our proposed reformulation, we remove the near-surface part of the model from the inversion and instead introduce an effective source to generate the wavefield at depth. This broadly requires that we replace the wavefield, u, and model, m, with versions including locations only below a chosen depth z^*: u^* and m^*, and that we introduce as an additional unknown a variable characterizing the wavefield after propagation through the near surface. This will require that we replace equation 1 (or its equivalent for other objective functions) with

$$\phi = \frac{1}{2}||R^*u^* - d^*||_2^2 \text{ subject to } C(m^*, u(z^*)) = 0, \tag{2}$$

where the * variables are equivalent to the corresponding terms in equation 1, but with positions and measurements above the chosen depth z^* removed. The specifics of the condition $C = 0$ in equation 2 differ based on how we choose to characterize the wavefield

from each source after propagating to z^* (now an additional unknown of our inversion problem). We outline in detail two possible choices for this characterization below.

Effective sources at depth

The first approach we discuss for characterizing the wavefield at depth z^* is to explcitly use an effective source at this depth. In this approach, we imagine a line source at z^* with appropriate amplitude, phase and moment tensor distribution along the line such that, when activated, it reproduces the same wavefield that would have been obtained by propagating the wavefield from a point source through the near-surface. By characterizing the problem in terms of this line source, we eliminate the need to solve the more difficult problem of characterizing the near surface. In this case, the VSP FWI optimization problem becomes

$$\min_{m^*,f^*} \frac{1}{2}||R^*u^* - d^*||_2^2 \text{ subject to } S^*(m^*)u^* = f^*. \tag{3}$$

Equation 3 is effectively the same optimization problem as conventional FWI, with the exception that we define the problem on a smaller model domain, and we invert for both an unknown model, m^*, and an unknown source term f^*. In order to represent arbitrary source moment tensors in a finite-difference simulation, f^* will generally need to be at least two grid cells thick, so in actuality, f^* will represent a set of multiple line sources around depth z^*. Simultaneous FWI for model and source properties has been discussed in detail in, for instance, Keating and Innanen (2020), so we do not derive in detail the expressions for the gradient and Hessian-vector product for this optimization problem, but we note that the computational cost of this inversion problem is about the same per iteration as for a conventional FWI. While this formulation is relatively straightforward and can make use of existing simultaneous source-model inversion techniques, it may not be easy to determine an optimal regularization or initialization for the source term f^* (we discuss this in detail later). For this reason, we consider also an alternative approach for wavefield characterization.

Wavefield at depth

A more direct, though slightly more difficult to implement, approach for characterizing the wavefield at depth z^* is to treat the wavefield itself as an inversion variable at the desired locations. This complicates the implementation of our condition that the wavefield be satisfied by forcing a change to the Helmholtz matrix. If the wavefield values at position indices n, u_n, are inversion variables, but the wavefield values at positions m are not, then we require a system of equations that allows us to specify u_n, but calculate u_m as a function of the model properties m. In this case, the VSP FWI optimization problem becomes

$$\min_{m^*,u_n} \frac{1}{2}||R^*u^* - d^*||_2^2 \text{ subject to } \begin{bmatrix} I \\ S_m(m^*) \end{bmatrix} u^* = \begin{bmatrix} u_n \\ 0 \end{bmatrix}, \tag{4}$$

where I is an identity matrix with a number of rows equal to the number of elements in u_n, and S_m includes only the rows of S^* corresponding to the depths in u_m. This formulation ensures that u_n can be directly manipulated by the inversion, and that $S^*(m^*)u_m = f_m$, where, in the VSP case, the source term f_m is a vector of zeros (as there will be no sources

below depth z^*). Just as multiple line sources were required in the effective source case to account for all moment tensors, multiple wavefield depths will have to be included in u_n to accurately represent downgoing wave propagation. Significantly, equation 4 is in a very similar form to equation 3, requiring an inversion for a source-like term and a subsurface model. In consequence, the gradients and Hessian-vector products required in FWI can be calculated for this formulation as a simultaneous source-model inversion (e.g. Keating and Innanen, 2020), just as in the effective source case. The only special consideration for this approach is that the derivatives of the Helmholtz matrix $\frac{\partial S}{\partial m}$ will be zero for the rows of S that have been replaced with the identity matrix.

Regularization

Both of the approaches suggested here have similar computational costs and similar numbers of inversion unknowns. While the computational cost of these approaches is about the same per iteration as for conventional FWI, the number of unknowns is generally significantly larger: instead of characterizing the near surface (requiring one unknown per depth per horizontal position), they characterize an effective source or wavefield at a given depth (requiring two unknowns per horizontal position, per source, per frequency). To provide some constraint on the extra variables, it is important to include a regularization term in the inversion. This regularization should provide additional information to the inversion about which possible wavefields are reasonable and which are not. Because our knowledge of a survey acquisition will inform us about which wavefields, rather than which effective sources reproducing those wavefields, are reasonable we will focus here on formulating appropriate regularization for the wavefield-based approach.

A key piece of information that is explicitly introduced in the conventional FWI formulation, but is not in our VSP FWI formulations is the location of the seismic source. By replacing propagation through an unknown near surface with inversion for a wavefield at depth, we also discard the explicit information about the source location. While the measured data should indirectly suggest the location of the source, it may be possible to improve inversion speed and accuracy by explicitly enforcing inversion penalty terms based on the expected spatial distribution of source energy. We make the assumption that, while propagation through the near-surface can cause redistribution of wavefield energy between modes and in time, there is limited lateral redistribution of the wavefield's energy. Based on this assumption, we define the inversion penalty term

$$\phi_R = \sum_s ||E_s(x) - (u_{x_s}^2(x) + u_{z_s}^2(x))||^2, \tag{5}$$

where $E_s(x)$ is the expected energy at position (x, z^*) based on the starting model for the inversion and the survey's source locations for shot s, u_{x_s} is the x-component of the wavefield for the sth shot, and u_{z_s} is the z-component of the wavefield for the sth shot. By including this term in the objective function, we ensure that the near surface is not treated as arbitrarily redistributing energy at depth z^*. This condition is merited in typical seismic surveys.

NUMERICAL EXAMPLES

To illustrate the effective source VSP FWI strategy we propose in this report, we present synthetic examples in this section. These examples make use of the wavefield-estimatation strategy, while the latter source estimation strategy is demonstrated in the companion reports Keating et al. (2021) and Eaid et al. (2021a).

Parameterization

In this report, we consider an elastic FWI approach in which strong correlations between the different elastic properties are assumed to be present. Based on this assumption, we frame the inversion in terms of a single parameter, γ, that specifies a corresponding p-wave velocity, s-wave velocity and density. This approach is motivated by the observation of a strong correlation between these variables at the CAMI field site, and is developed and discussed in more detail by Eaid et al. (2021b). The key feature of this approach for the synthetic examples presented here is that it allows for a single-parameter elastic FWI approach, and eliminates concerns about cross-talk. In the synthetic examples presented here, the true models used to generate the 'measured' data are consistent with this single-variable parameterization.

In both our synthetic modeling and inversion, we use the elastic, frequency-domain finite difference modeling approach of Pratt (1990).

Layer model

In our first synthetic example, we consider a one-dimensional layer model, shown for P-wave velocity, v_P in Figure 1. Our objective in this test is to invert for this model using the wavefield estimation method, rather than explicitly recover the top part of the model. So, even though the near-surface is not highly complex in this synthetic case, we use this example to test the properties of the inversion when it is replaced with a wavefield estimate. The initial model we use for this example is a homogeneous medium with the properties of the top layer of the true model. We consider 23 explosive sources along the top of the model at intervals of 10 m and 100 receivers from depth 2.5 m to 250 m, with an x-position of 0, representing down-hole geophones.

For this example, we invert for an effective source at 40 m depth, and consider the model above this depth to be part of the near-surface. We initialize the wavefield at 40 m by using the modeled wavefield from the initial model at this depth. We consider a one-dimensional inversion here, so the inversion variables for the subsurface model consists of layer-parameterizing variables. Our method for changing the spatial basis functions of the inversion follows Keating et al. (2018). To prevent unwanted interaction with the source term, the model is only updated at depths more than eight finite-difference grid-cells (20 m) below the effective source depth.

We consider seven frequency bands of eight frequencies in this inversion, with each band including frequencies from 1 Hz (the lowest frequency considered) to an upper bound equal to 4.5 Hz at the lowest (and first) band, and increasing to 30 Hz at the highest (and

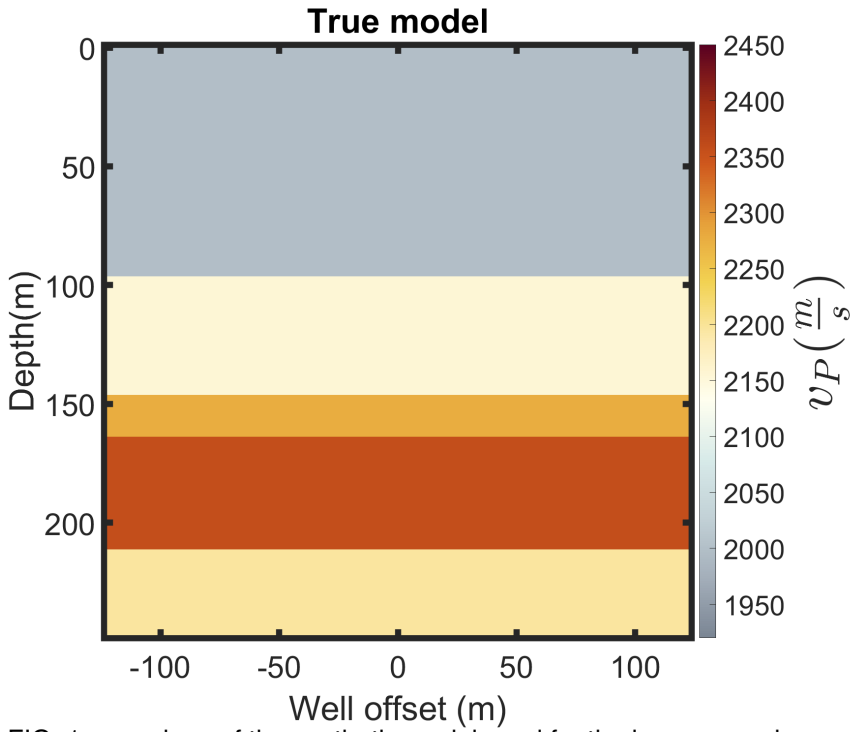

FIG. 1. v_P values of the synthetic model used for the layer example.

last) frequency band. Starting from the initial model and wavefield estimate, we perform 30 iterations of L-BFGS optimization per frequency band.

The inverted P-wave velocity model for the 1-D example is shown in Figure 2. This result has several positive qualities: it correctly recovers a sharp contrast at depths corresponding to each of the four layer interfaces in the true model, it identifies that each of the layers has a larger v_P than the initial model, and it correctly identifies the velocity decrease between the fourth and fifth layers. Several prominent flaws are also evident in this inversion result. There is a persistent oscillation in velocities in the second and third layers (approximately 100-160 m) that is not present in the true model, and these oscillations introduce contrasts of similar magnitude to that between the second and third layers. This makes the layering structure of the true model unclear in the inversion. The inverted model also fails to recover accurate amplitudes for the changes from the initial model, significantly underestimating the v_P values in the fourth and fifth layers.

Block model

For a second synthetic example, we consider a case with two-dimensional structures, with some major features far from the VSP well. The true model for this example is shown in Figure 3, and consists of rectangular anomaly regions in an otherwise constant background medium. For this example we use acquisition geometry, finite-difference grid and effective source depth equal to the parameters chosen in the first example. The frequency bands used and optimization strategy are also the same as in the previous case.

Instead of a layer-based parameterization for the subsurface model, we use spatial

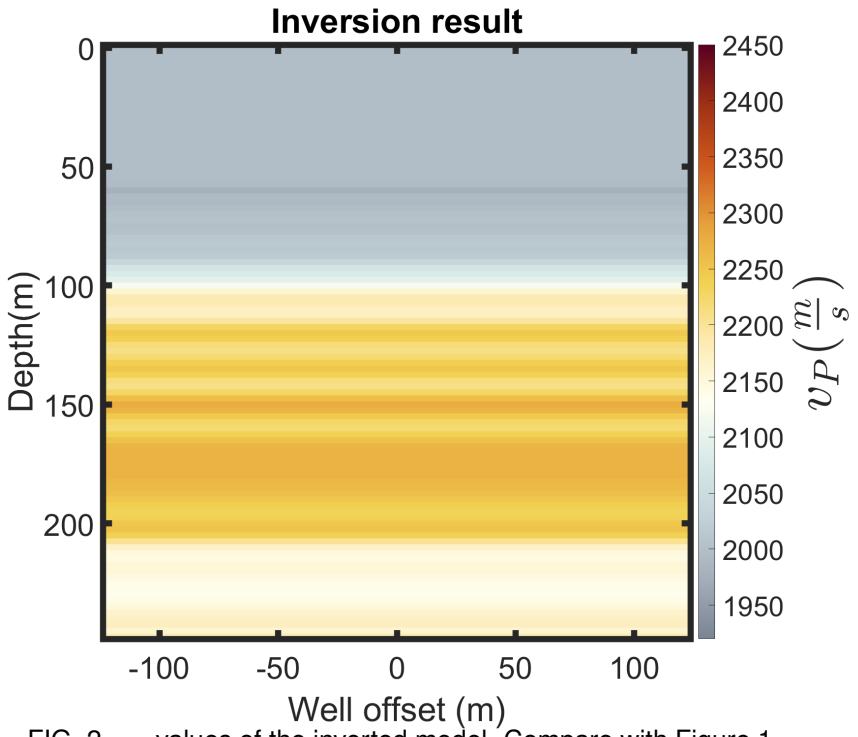

FIG. 2. v_P values of the inverted model. Compare with Figure 1.

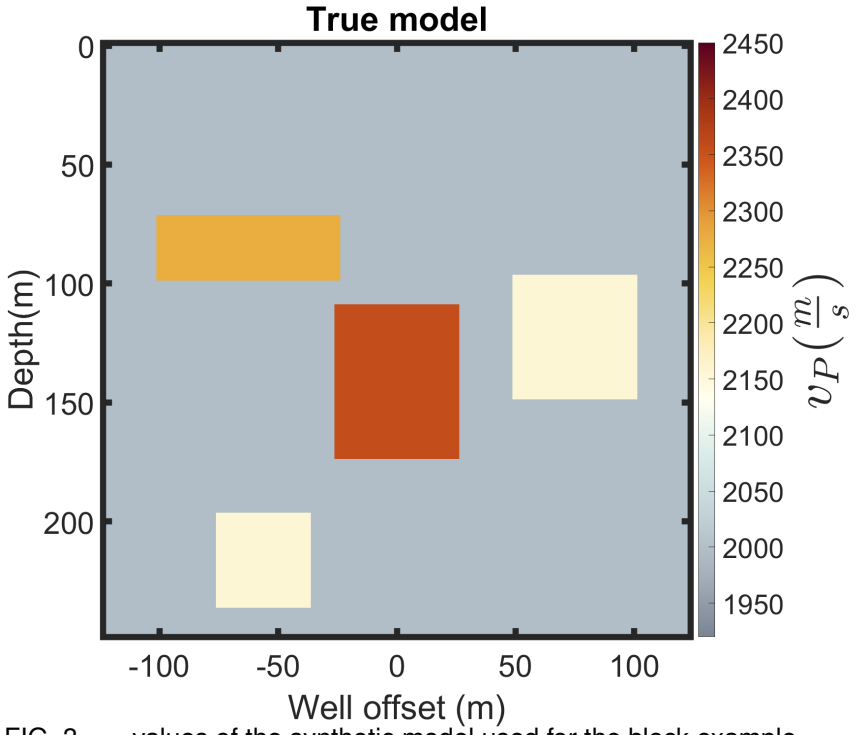

FIG. 3. v_P values of the synthetic model used for the block example.

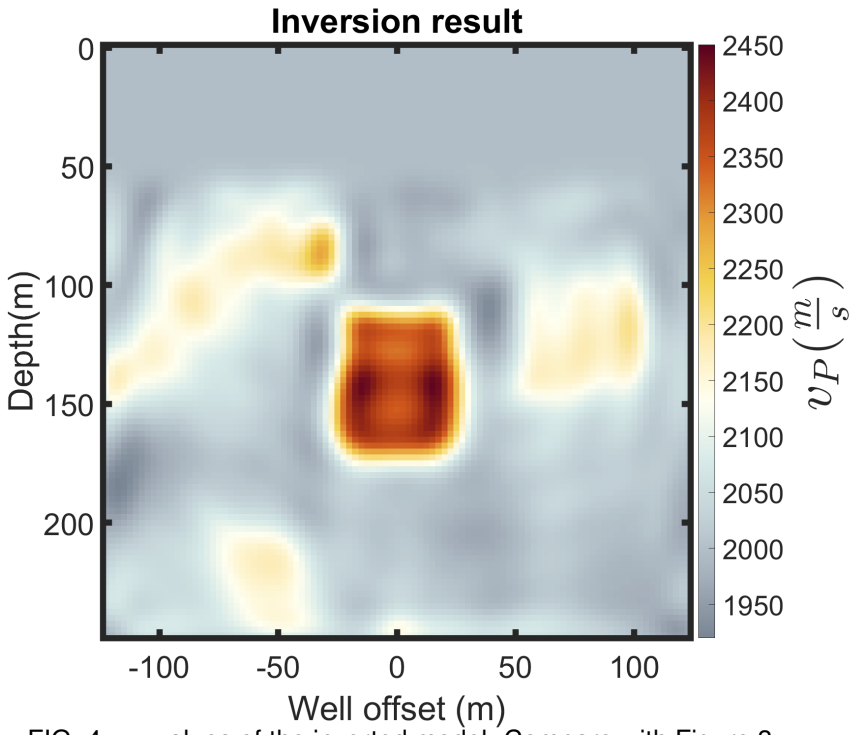

FIG. 4. v_P values of the inverted model. Compare with Figure 3.

Gaussian functions with a standard deviation of three grid cells as the basis function for this inversion. This small, smooth basis function helps to prevent the near-well grid cells (where the impact on the measured data is the largest) from recovering very different values than their surroundings.

The inverted v_P model for the block model example is shown in Figure 4. In this case, the inversion successfully identifies each of the four blocks present in the true model. The block centered on the well is the most accurately recovered and the block on the right-hand side of the model is also recovered well. The blocks on the left-hand side are less accurately recovered; the shallow block on the left is somewhat accurate near the well, but very poorly characterized further away. This is likely due to the relatively poor coverage away from the well and the predominance of transmission raypaths for characterizing this shallow block. An anomalous low-velocity region is also recovered in the inversion on the left-hand side and not present in the true model, but this feature appears in a region of very poor data coverage. This ringing features present in the layer model example seem absent in this case.

DISCUSSION

In both of the synthetic examples considered, the inverted model was able to recover some of the key features of the true model, despite replacing the known source characteristics and near surface with an unknown effective wavefield at depth. This suggests that this approach is a viable candidate for coping with field data where the source and near surface are complex and unknown. This robustness may be associated with other disadvantages, and we plan to investigate in detail how the results of this approach compare to a

conventional inversion strategy in future work.

While we consider a frequency-domain implementation of this approach here, a time-domain version may have significant advantages. In particular, we are primarily interested in capturing the behaviour of the downgoing wavefield in our estimate of the effective source in this approach, but the frequency-domain implementation makes this distinction difficult to enforce, and in this report, we invert for the entire wavefield at the cutoff depth. This means that the source we have to invert for includes both downgoing energy from the source (directly related to the model features we choose to replace) and the upgoing energy resulting from reflections (more closely related to the part of the model we focus on in the inversion). This procedure may be more challenging due to the inclusion of difficult to characterize reflections, necessitated by the frequency-domain implementation. In the time domain, by characterizing the wavefield only for certain time ranges, this problem could simplified by both focusing on the downgoing portion of the wavefield and reducing the size of the wavefield variables to be inverted for.

CONCLUSIONS

In this report, we proposed an FWI approach for VSP data that replaced the problem of characterizing the near-surface with the problem of characterizing its effect on the seismic wavefield. As the latter relates much more directly to seismic data, this helps to simplify the VSP FWI problem. We proposed both source-based and wavefield-based implementations of this approach, and demonstrated that both can formulated as simultaneous source-model inversion problems, with comparable per-iteration computational cost to conventional FWI. To help ameliorate difficulties associated with the increased dimensionality of our approach, we proposed regularization terms to help restrict the recovered wavefields to reasonable values. We presented two numerical examples and demonstrated that an effective-source approach was capable of removing the near-surface from the problem, while accurately recovering key features of synthetic models. Field data implementations of this approach are detailed in the companion reports Keating et al. (2021) and Eaid et al. (2021a).

ACKNOWLEDGEMENTS

The authors thank the sponsors of CREWES for continued support. This work was funded by CREWES industrial sponsors and NSERC (Natural Science and Engineering Research Council of Canada) through the grant CRDPJ 543578-19. Matt Eaid was partially supported by a scholarship from the SEG Foundation. Scott Keating was also supported by the Canada First Research Excellence Fund, through the Global Research Initiative at the University of Calgary.

REFERENCES

Brossier, R., Operto, S., and Virieux, J., 2015, Velocity model building from seismic reflection data by full-waveform inversion: Geophysical Prospecting, **63**, 354–367.

Eaid, M., Keating, S., and Innanen, K. A., 2021a, Full waveform inversion of das field data from the 2018 cami vsp survey: CREWES Annual Report, **33**.

Eaid, M., Keating, S., and Innanen, K. A., 2021b, Processing of the 2018 cami vsp survey for full waveform

inversion: CREWES Annual Report, **33**.

Keating, S., Eaid, M., and Innanen, K. A., 2021, Full waveform inversion of vsp accelerometer data from the cami field site: CREWES Annual Report, **33**.

Keating, S., and Innanen, K. A., 2020, Simultaneous recovery of source locations, moment tensors and subsurface models in 2d fwi: CREWES Annual Report, **32**.

Keating, S., Li, J., and Innanen, K. A., 2018, Viscoelastic fwi: solving for q_p, q_s, v_p, v_s, and density: CREWES Annual Report, **30**.

Pratt, R. G., 1990, Frequency-domain elastic wave modeling by finite differences; a tool for crosshole seismic imaging: Geophysics, **55**, No. 5, 626–632.